Integration of Mobile Wind Sensor for Sensing Methane Emissions from Oil and Gas Infrastructure

2021 Mech 498: Research practicum

Presented by: Bilal Khan

Academic advisor: Dr. Azer P. Yalin Committee member Dr. Shantanu Jathar Graduate Student Mentor: Anthony Puga

Department of Mechanical Engineering, Colorado State University, Fort Collins, Colorado;

CENTER FOR LASER SENSING AND DIAGNOSTICS

Colorado State University

Atmospheric Methane

Sources

- Natural (permafrost, wildfires, freshwater) and anthropogenic (agriculture, oil and gas)

Benefits

- 'Clean' fuel compared to coal and gasoline, produces less CO_2 after from combustion

Impacts

- Greenhouse gas (37x stronger than CO_2)
- Contributes towards ozone formation
- Affects atmospheric oxidation through reactions with *OH radical

Fugitive Oil and Gas Emissions

- Increase in natural gas extraction for use of methane as a 'clean' combustion fuel, EPA estimated >500k gas and >500k oil wells in the US in 2011
- Extraction includes extensive networks of wells, pipelines, and processing facilities, which all have the potential for small gas leaks
- Estimates of methane emissions due to leaks have been performed looking at different components and scales of the industry from local direct measurements to top-down aircraft studies
- Portable analyzers prove extremely useful for locating and measuring leaks

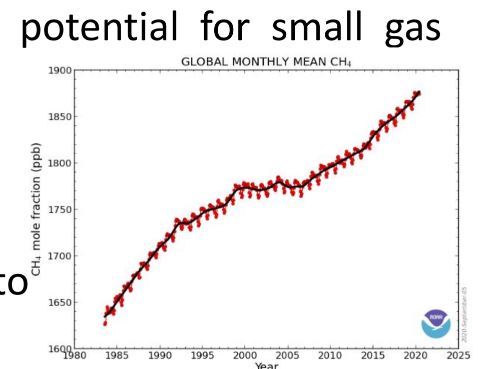

National Oceanic and Atmospheric Administration Global CH4 Monthly Means (2020)

Current Emissions Monitoring Approaches

- Imaging cameras (inefficient)
- Satellite, airplanes (insensitive)
- *Mobile sampling with trucks or UAVs. Wind from stationary sensor.*

Albertson et al. (2016)

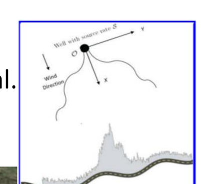

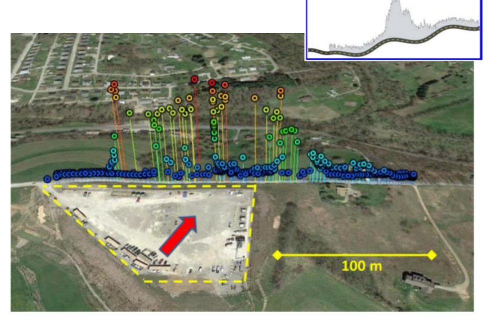

Multiple passes along a road next to oil and gas infrastructure McHale et al. (2019)

Stationary Wind Sensor Shortcomings

- Bulky setup which makes it difficult to relocate
- Less accurate and reliable as it has to be setup away from the truck

Wind Significance

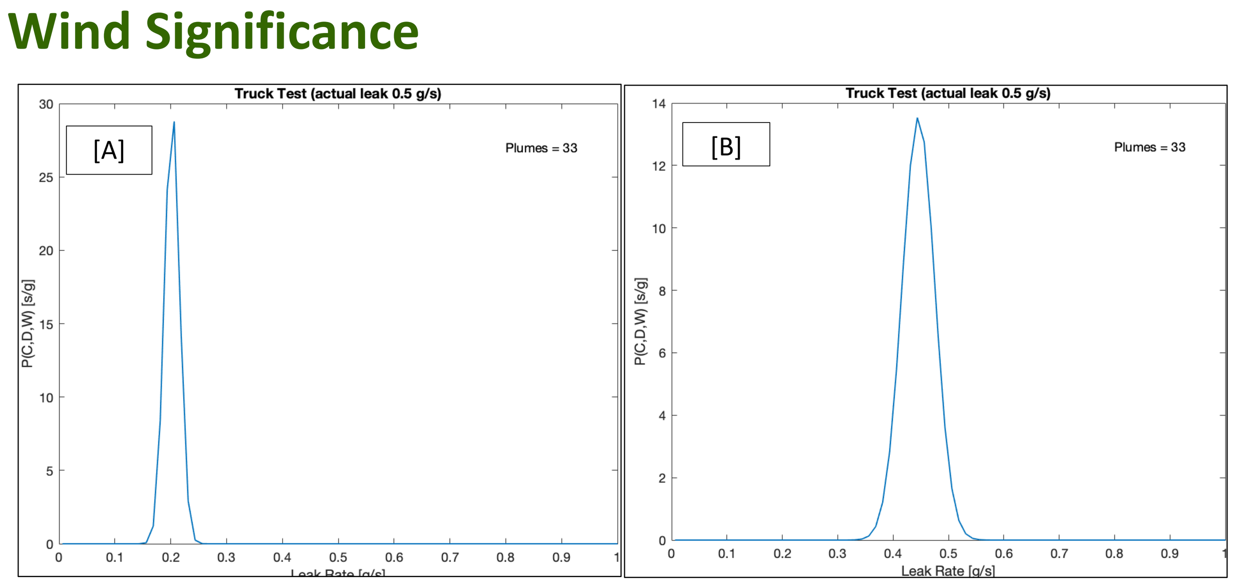

The importance of wind (Probability density function)

- In [A] only the final 1/3 of the wind data was collected where as [B] is from a test with complete and stable
- Better wind data collection resulted in much better inference of the leak rate of 0.5 g/s

Gill Ultrasonic Anemometer www.gillinstruments.com

Mobile WindSonic Anemometer

- No moving parts, compact, and light weight
- Corrosion-free polycarbonate housing
- -35°C to +70°C
- 300 mm/hr precipitation rate
- 0-60 m/s wind speed
- 0-359º wind direction
- 1 Hz sampling rate

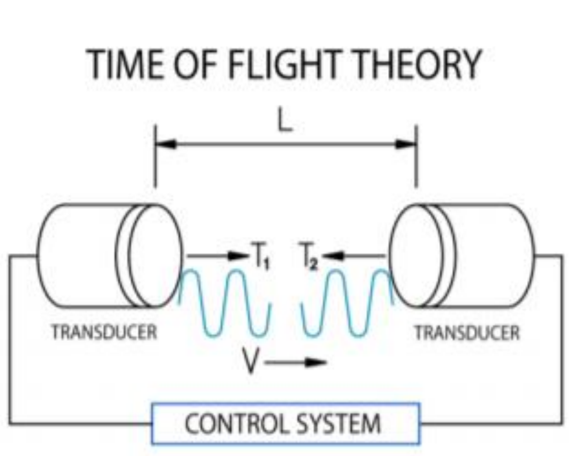

Ultrasonic pulse www.gillinstruments .com

Operating Principle

- Four transducers for the four cardinal directions
- Ultrasonic pulses are sent between opposite transducers and the time it takes for them to travel that distance is noted
- The difference in the times of flight on each axis can be used to calculate the wind speed and direction

Setup and Methods

- Designed and fabricated a mounting mechanism for the mobile wind sensor using a couple of steel L brackets and a PVC pipe. The pipe allows for the height of the wind sensor to be altered for different testing heights.
- Developed stationary sensor and mobile sensor data sharing protocols.
- Outdoor stationary tests showed good agreement between the new mobile wind sensor and the stationary wind sensor.
- Multiple heights above the truck were tested to find the optimum starting height for the tests.
- Haversine formula was used to convert geospatial coordinates to velocity readings by dividing the distance between two coordinates by the sampling time.

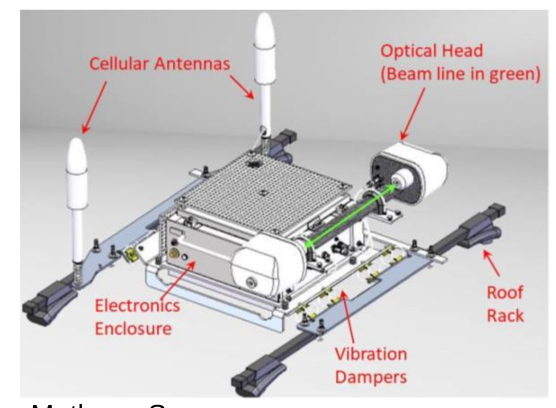

Methane Sensor

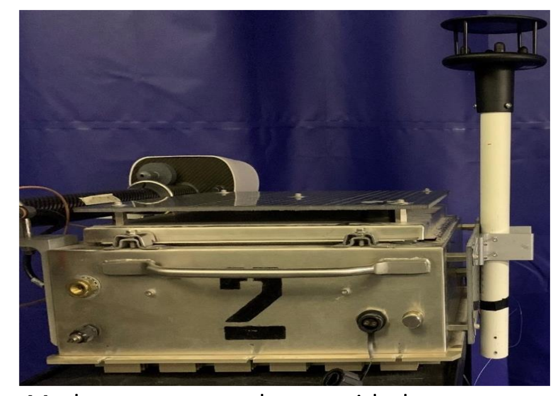

Methane sensor enclosure with the mount.

Distance Calculation

$$a = \sin^2(\Delta\phi/2) + \cos\phi_1 \cdot \cos\phi_2 \cdot \sin^2(\Delta\lambda/2)$$

$$c = 2 \cdot \operatorname{atan2}(\sqrt{a}, \sqrt{1-a})$$

$$d = R \cdot c \quad \text{(Equation 1)}$$

ϕ is latitude, λ is longitude, R is earth's radius (mean radius = 6,371km), and d is the distance. All the angles need to be in radians.

Bearing Calculation

$$\theta = \operatorname{atan2}(\sin\Delta\lambda \cdot \cos\phi_2, \cos\phi_1 \cdot \sin\phi_2 \ldots - \sin\phi_1 \cdot \cos\phi_2 \cdot \cos\Delta\lambda) \quad \text{(Equation 2)}$$

ϕ_1,λ_1 is the start point, ϕ_2,λ_2 is the end point, Δλ is the difference in longitude and θ is the bearing angle

True Wind Calculation Protocol

$$\vec{v}_{tw} = \vec{v}_a - \vec{v}_v \quad \text{(Equation 3)}$$

$\vec{v}_{tw}$ is the true wind, $\vec{v}_a$ is the measured wind velocity from the anemometer, and $\vec{v}_v$ is the vehicle velocity.

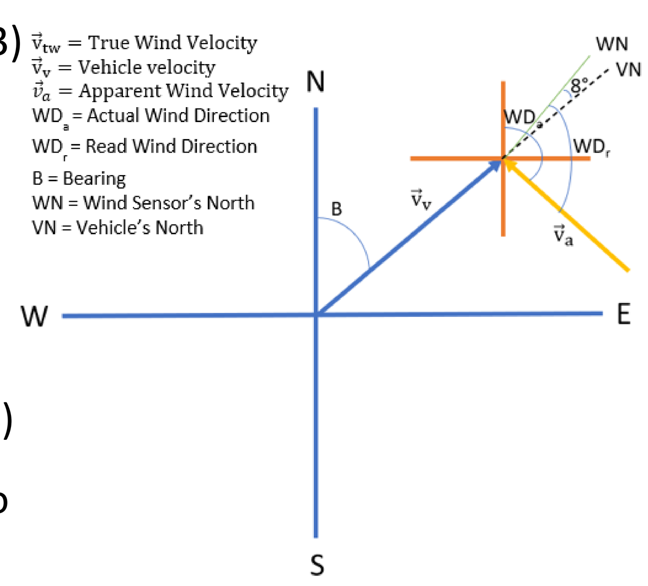

Actual Wind Direction

$$WD_a = B + WD_r - 8° \quad \text{(Equation 4)}$$

Variables are defined in the figure to the right

True Wind

$$\vec{v}_{tw} = (\cos(WD_a)*|\vec{v}_a|-\cos(B)*|\vec{v}_v|)\hat{\imath} + (\sin(WD_a)*|\vec{v}_a|-\sin(B)*|\vec{v}_v|)\hat{\jmath} \quad \text{(Equation 5)}$$

Variables are defined in the figure to the right

Mobile Field Tests for True Wind Calculation

- Multiple tests were conducted to find the optimum height of the wind sensor above the vehicle.
- Christman airfield was chosen as the testing site because it does not have any large infrastructure around it which could have acted as a source of potential noise in the experiments.

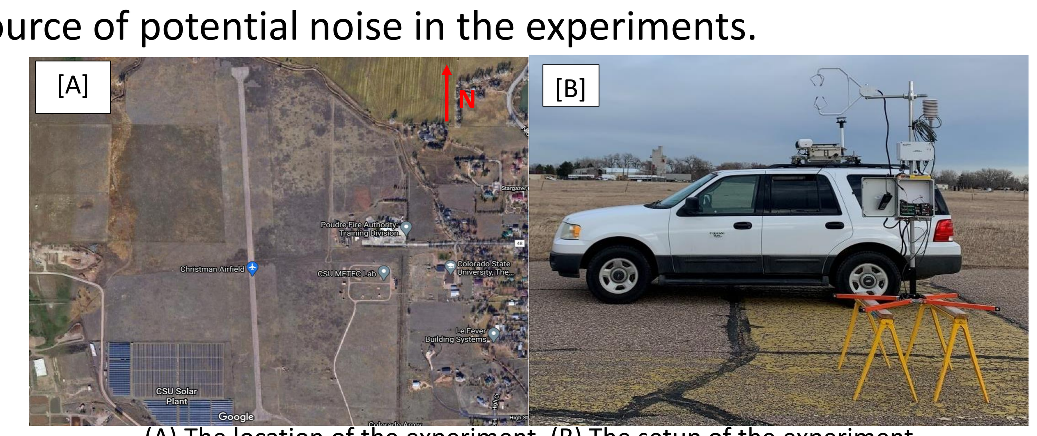

(A) The location of the experiment. (B) The setup of the experiment.

- The results were averaged by track run. No turning points were considered for the tests to strengthen the accuracy of the system. The results from one such test are shown below. The bearing and speed of the vehicle were maintained constant over every single track run.

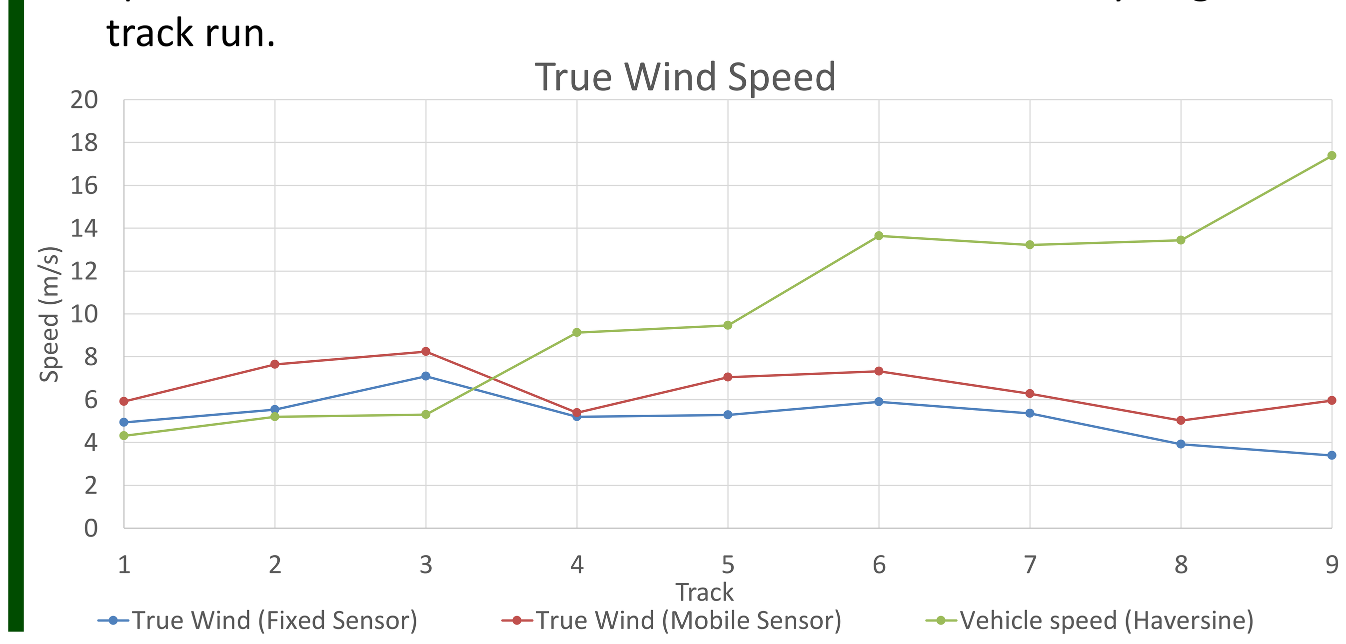

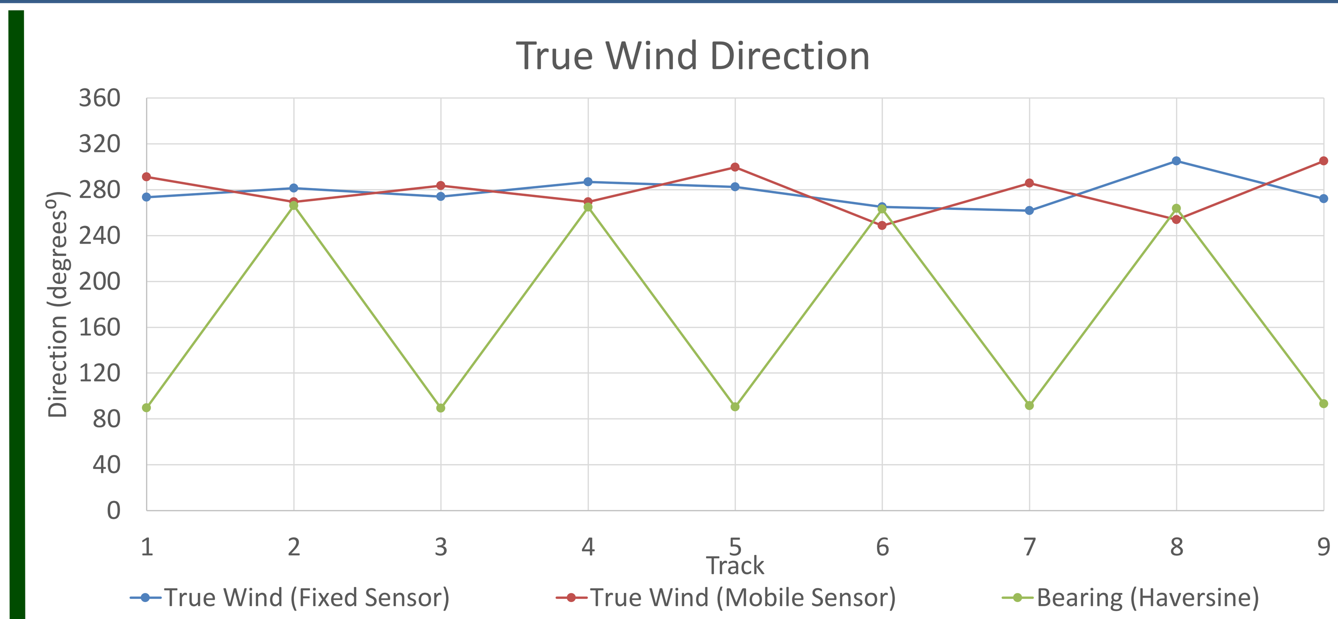

- The results from this particular test showed good agreement between the actual wind speed and direction. This could be because of the high actual wind speed.

Errors

- There is a general trend that as the vehicle speed increases, the calculated true wind has a higher error percentage in its magnitude and direction.
- At higher vehicle speeds, the apparent wind is dominated mostly by the motion of the car itself due to which the percentage error increases.
- Higher actual wind speeds resulted in lower errors in the final calculation. Tests where actual wind speed's been higher than 5 m/s have given better results.
- The error graphs below are a compilation of 3 different tests conducted in different wind conditions which show these trends in the error.

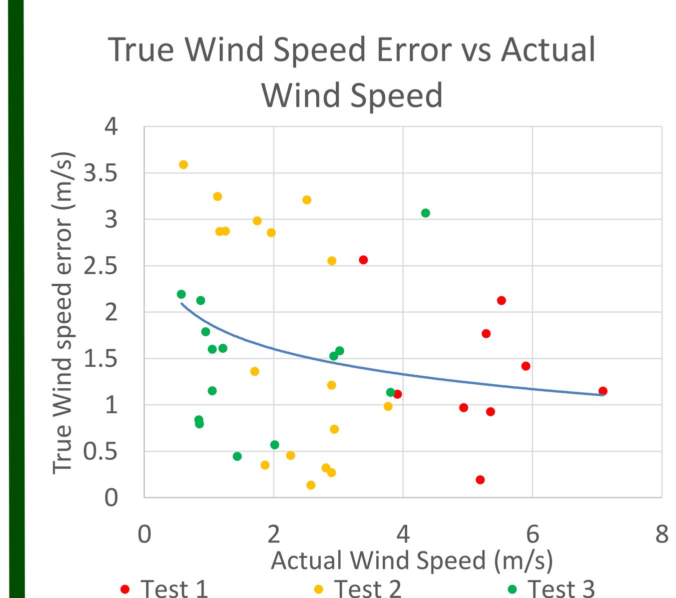

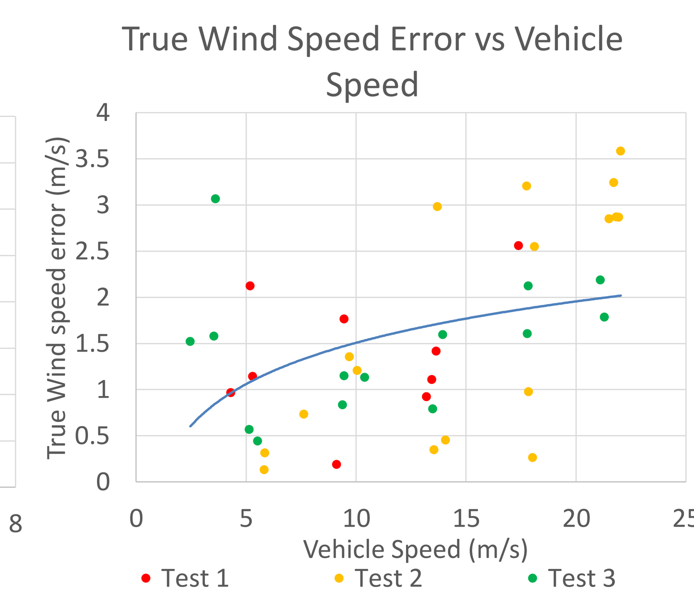

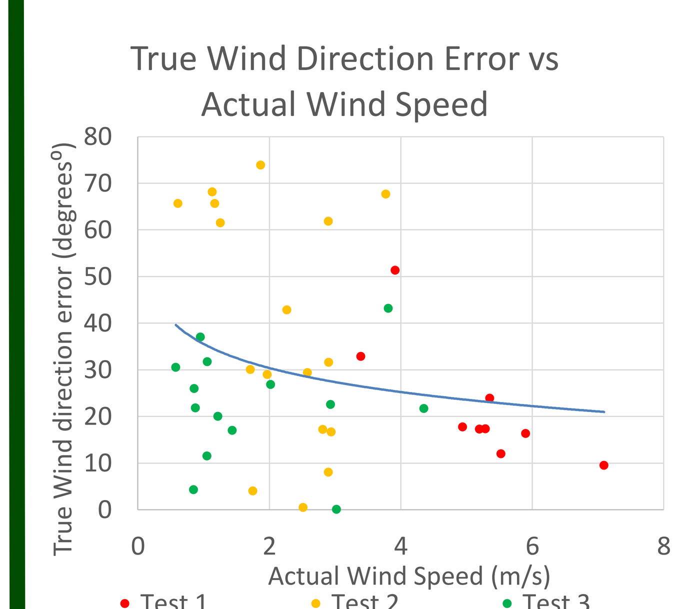

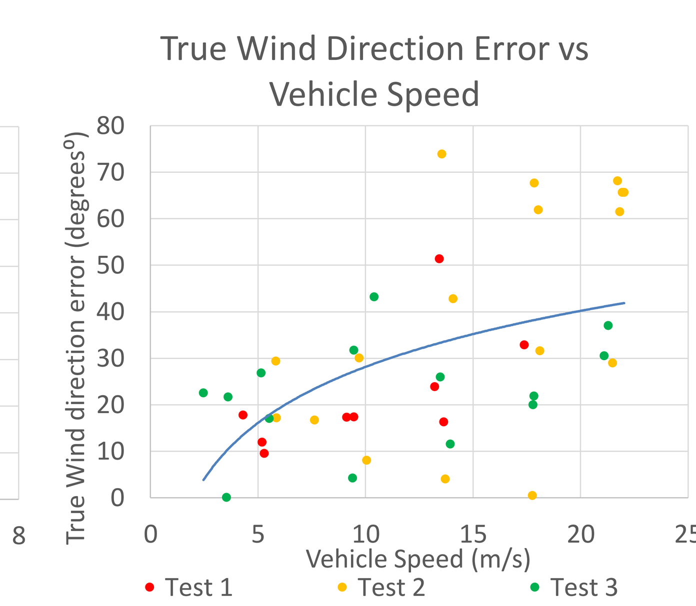

Future Work

- Further field tests are required to understand the error sources in the true wind better. Testing will be repeated till the obtained results consistently show higher accuracy and reliability.
- Multiple mounting locations at varying heights on the truck can be tried to minimize the effects of the perturbed flow of air around the car.

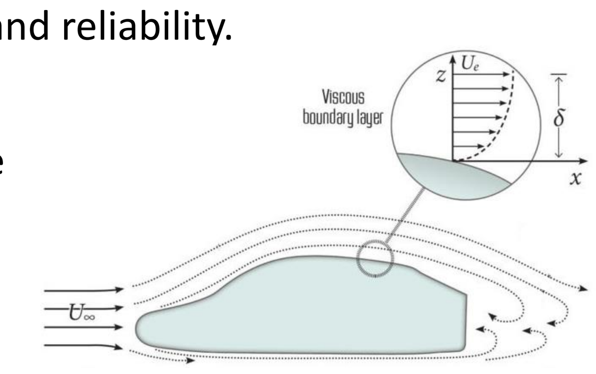

- Develop calculation protocol for the determination of quantitative emission detection.
- Outdoor methane release and detection: Controlled outdoor methane release and mobile detection to investigate sensitivity of measurements for leak detection.
- Fugitive leak detection: Measure methane near various oil and gas facilities to look for actual fugitive methane leaks which would help improve estimates of methane emissions and let operators know of issues.

Contact Information

- **Bilal Khan, CENTER FOR LASER SENSING & DIAGNOSTICS, Dept. Mechanical Engineering, Colorado State University, bilalk@rams.colostate.edu 970-818-6228**

References

L. E. Mchale, B. Martinez, T. W. Miller, and A. P. Yalin, "Open-path cavity ring-down methane sensor for mobile monitoring of natural gas emissions," *Opt. Express*, vol. 27, no. 14, p. 20084, Jul. 2019, doi: 10.1364/OE.27.020084.

John. D. Albertson *et al.*, "A Mobile Sensing Approach for Regional Surveillance of Fugitive Methane Emissions in Oil and Gas Production," *Environ. Sci. Technol.*, vol. 50, no. 5, pp. 2487–2497, Mar. 2016, doi: 10.1021/acs.est.5b05059.

www.gillsinstruments.com